Electronic Supplementary Material (ESI) for Journal of Materials Chemistry A.

Supporting Information

Spiro-OMeTAD or CuSCN as a preferable hole transport material for carbon-based planar perovskite solar cells?

Yang Yang, Minh Tam Hoang, Disheng Yao, Ngoc Duy Pham, Vincent Tiing Tiong, Xiaoxiang Wang, Hongxia Wang *

School of Chemistry, Physics and Mechanical Engineering, Science and Engineering Faculty, Queensland University of Technology, Brisbane 4001, Australia

*Corresponding Author.

E-mail address: hx.wang@qut.edu.au (H.X. Wang).

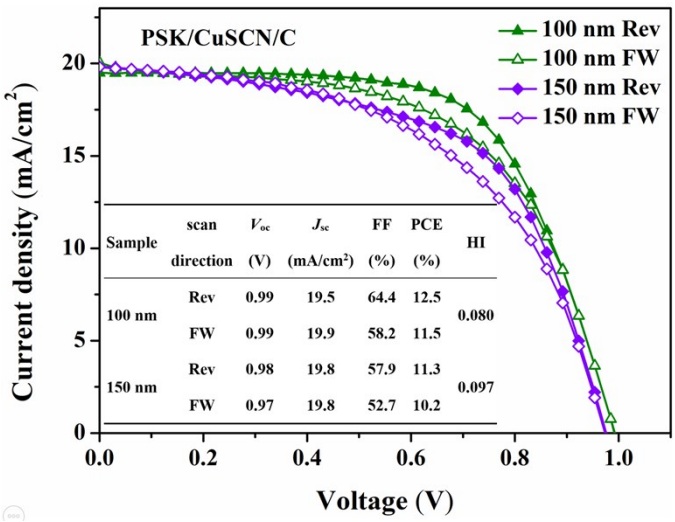

Figure S1. *J-V* curves of the PSK/CuSCN/C with different thickness of CuSCN layer under reverse and forward scans.

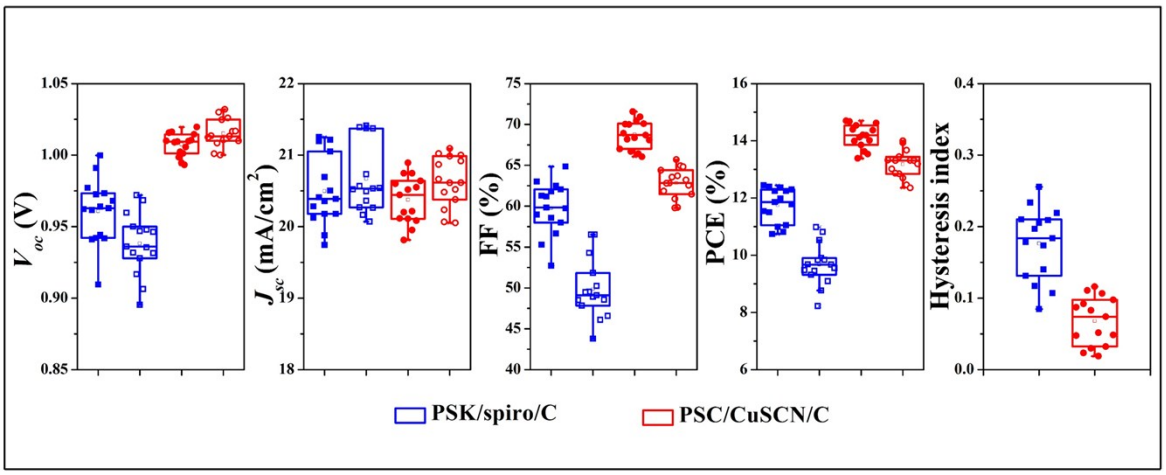

Figure S2. Statistical photovoltaic parameters for 15 cells based on spiro-OMeTAD and CuSCN with an illumination area of 0.115 cm^2 under both reverse and forward scan.

Table S1. Photovoltaic parameters for 15 cells based on spiro-OMeTAD and CuSCN measured under 1 sun illumination condition at both reverse and forward scans.

sample	scan direction	V_{oc} (V)	J_{sc} (mA/cm^2)	FF (%)	PCE (%)	HI[a]
PSK/spiro/C	Rev	0.96 ± 0.02	20.5 ± 0.5	59.8 ± 3.1	11.7 ± 0.6	0.176 ± 0.048
	FW	0.94 ± 0.02	20.7 ± 0.5	49.8 ± 3.5	9.7 ± 0.7	
PSK/CuSCN/C	Rev	1.01 ± 0.01	20.4 ± 0.3	68.8 ± 1.7	14.1 ± 0.4	0.068 ± 0.033
	FW	1.02 ± 0.01	20.6 ± 0.3	62.8 ± 1.7	13.2 ± 0.5	

[a]Hysteresis index = $(PCE_{Rev} - PCE_{FW})/PCE_{Rev}$

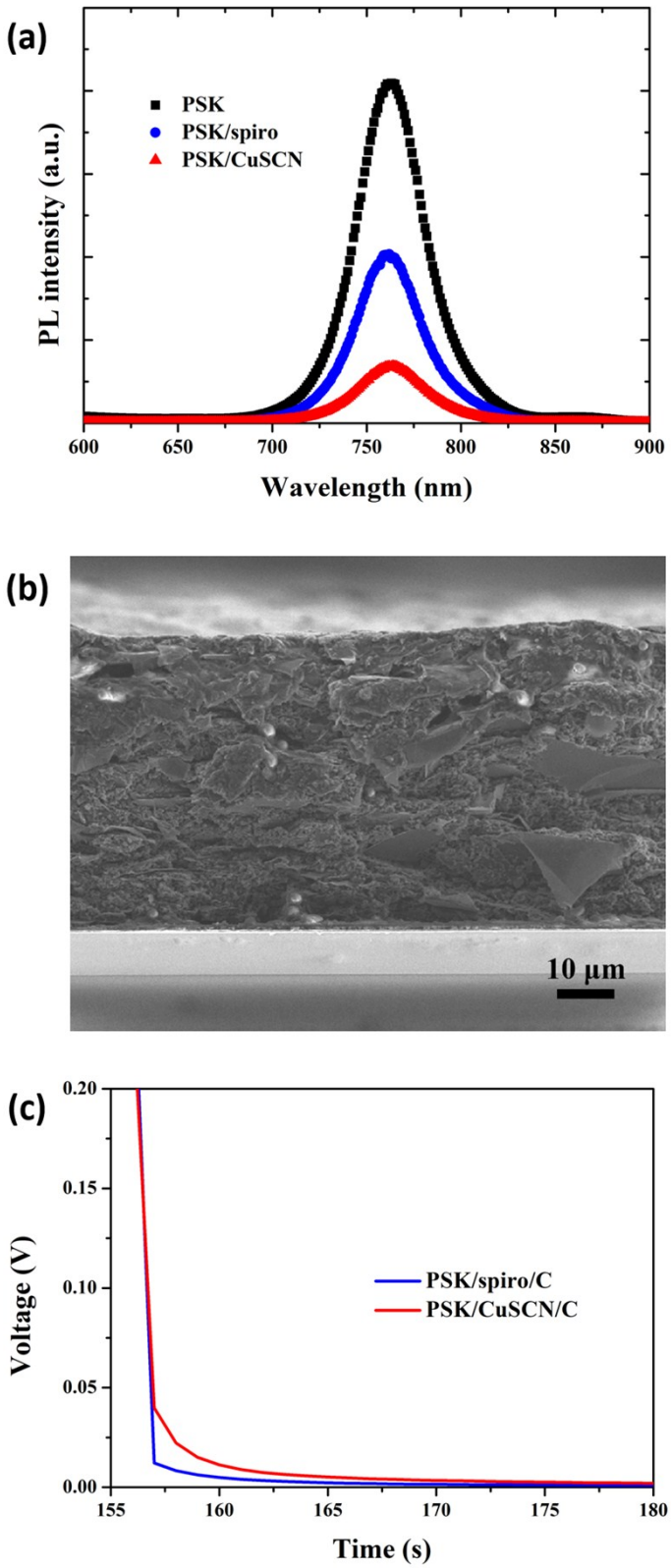

Figure S3. (a) Steady-state PL spectrum of various films and the excitation wavelength is 487 nm. (b) Cross-sectional SEM image of carbon film on the device. (c) Zoomed-in plot of *Voc* response at the end of the first illumination cycle.

Table S2. Characteristic photovoltaic parameters of PSCs measured under 1 sun illumination condition at different scan rates.

sample	scan rate	scan direction	V_{oc} (V)	J_{sc} (mA/cm^2)	FF (%)	PCE (%)	HI[a]
PSK/spiro/C	300 mV/s	Rev	0.94	20.9	61.6	12.1	0.273
		FW	0.92	20.9	45.7	8.8	
	200 mV/s	Rev	0.95	20.8	61.8	12.2	0.197
		FW	0.92	20.9	50.6	9.8	
	140 mV/s	Rev	0.94	20.7	60.0	11.5	0.087
		FW	0.94	20.7	54.3	10.5	
	50 mV/s	Rev	0.95	20.7	59.9	11.8	0.110
		FW	0.93	20.8	54.3	10.5	
	14 mV/s	Rev	0.95	20.8	60.6	12.0	0.142
		FW	0.93	20.8	53.5	10.3	
PSK/CuSCN/C	300 mV/s	Rev	1.00	21.2	68.9	14.6	0.062
		FW	1.01	21.3	63.6	13.7	
	200 mV/s	Rev	1.00	21.0	66.4	13.9	0.022
		FW	1.01	21.3	63.3	13.6	
	140 mV/s	Rev	1.00	20.9	66.3	13.9	0.036
		FW	1.01	21.3	62.8	13.4	
	50 mV/s	Rev	1.00	20.9	67.1	14.0	0.021
		FW	0.99	21.0	65.9	13.7	
	14 mV/s	Rev	1.00	20.8	68.8	14.3	0.035
		FW	0.97	20.9	67.9	13.8	

[a]Hysteresis index = $(PCE_{Rev} - PCE_{FW})/PCE_{Rev}$

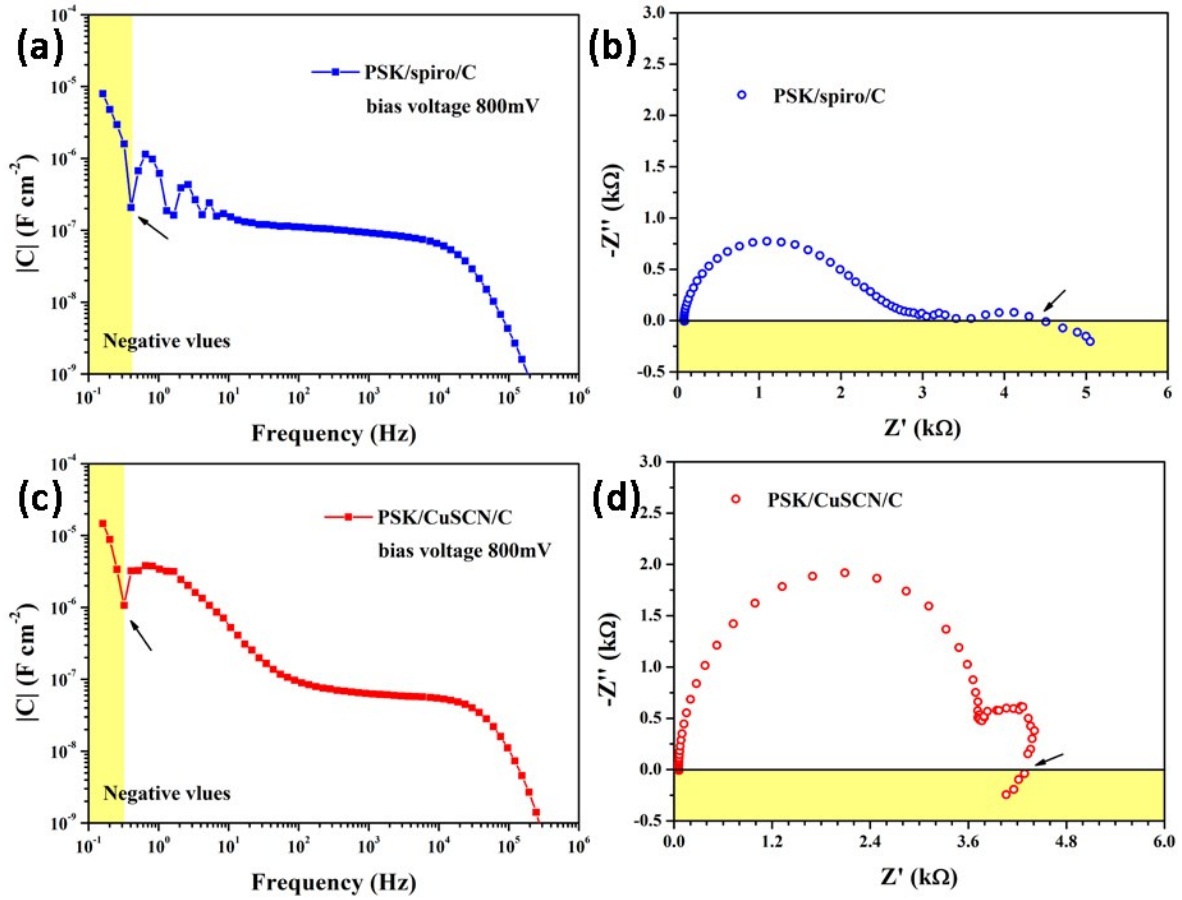

Figure S4. Absolute values of capacitance as a function of frequency obtained in the dark at 800 mV bias for (a) PSK/spiro/C and (c) PSK/CuSCN/C. The corresponding impedance spectroscopy spectrum for (b) PSK/spiro/C and (d) PSK/CuSCN/C.

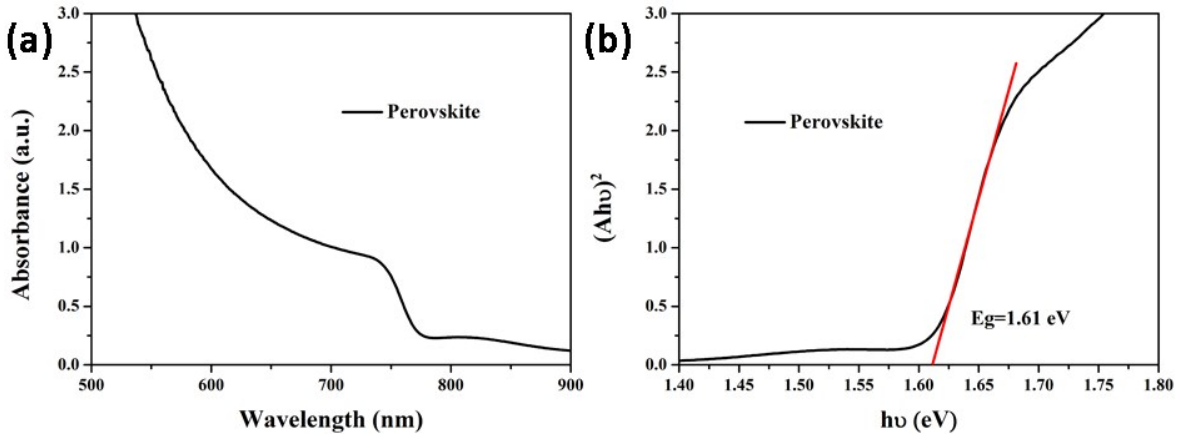

Figure S5. (a) UV-vis absorption spectra of triple cation perovskite film. (b) Evolution of optical band gap of perovskite film according to the absorbance spectrum.

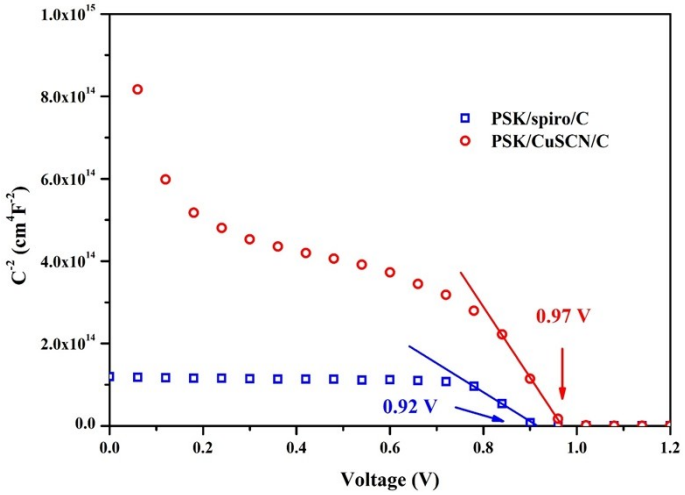

Figure S6. Capacitance as a function of voltage bias in the Mott-Schottky plot for PSK/spiro/C and PSK/CuSCN/C, respectively.

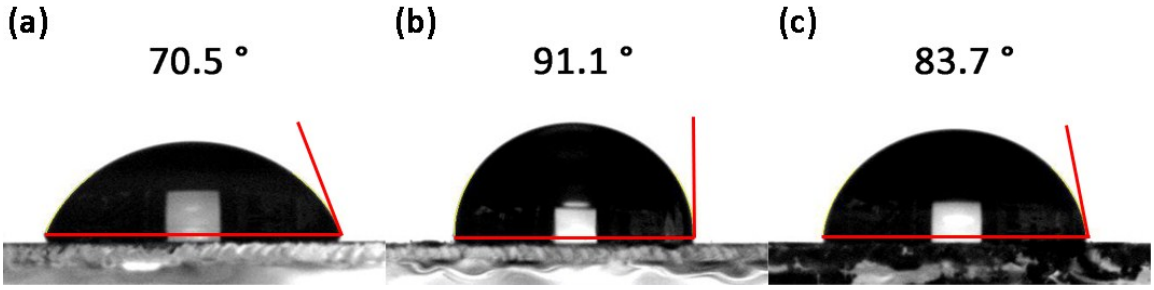

Figure S7. Characterization of the wettability of (a) triple cation perovskite layer, (b) spiro-OMeTAD layer and (c) CuSCN layer measured at 60 s after water droplet deposition.

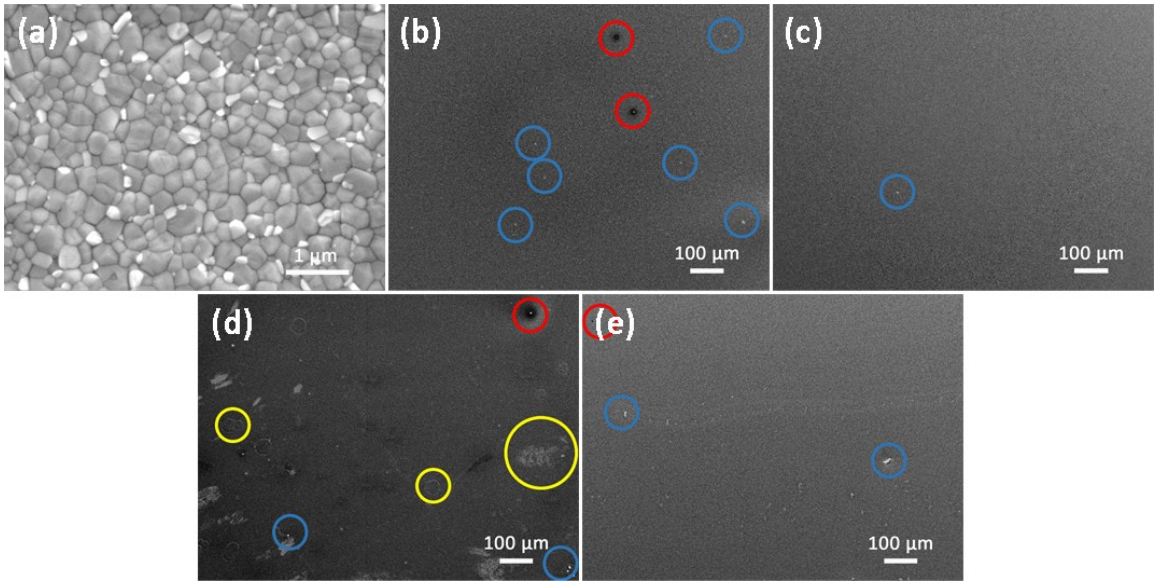

Figure S8. Top-view SEM images of fresh (a) triple cation perovskite film (b) spiro-OmeTAD layer on perovskite film and (c) CuSCN layer on perovskite film, (d) spiro-OmeTAD layer and (e) CuSCN layer aging for 80 days (humidity: 55-70%). Particles, holes and exposed area are in red, blue and yellow circles, respectively.

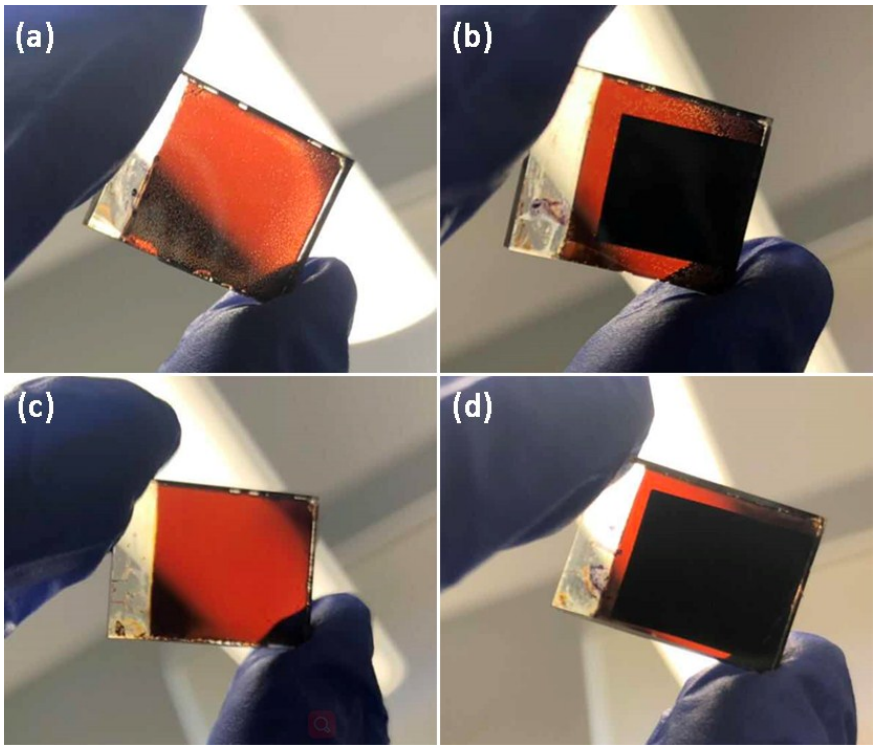

Figure S9. Digital images of (a) spiro-OMeTAD coated on perovskite, (b) PSK/spiro/C, (c) CuSCN coated on perovskite and (d) PSK/CuSCN/C aging for 80 days stored in ambient condition (relative humidity: 55-70%).